Hamiltonian Map Description of Electron Dynamics in Gyrotrons

Olgierd Dumbrajs, *Senior Member, IEEE*, Yannis Kominis, Konstantinos A. Avramides, Kyriakos Hizanidis, and John L. Vomvoridis

***Abstract*—Electron dynamics in gyrotron resonators are described in terms of a Hamiltonian map. This map incorporates the dependency of electron dynamics on the parameters of the interacting radio-frequency (RF) field and it can be used for trajectory calculations through successive iteration, resulting in a symplectic integration scheme. The direct relation of the map to the physics of the model, along with its canonical form (phase space volume preserving) and the significant reduction of the number of iteration steps required for acceptable accuracy, are the main advantages of this method in comparison with standard methods such as Runge–Kutta. The general form of the Hamiltonian map allows for wide applications as a part of several numerical algorithms which incorporate CPU-consuming electron trajectories calculations.**

***Index Terms*—Gyrotrons, Hamiltonian mappings, microwave sources, symplectic integration.**

I. Introduction

GYROTRONS are microwave sources whose operation is based on the stimulated cyclotron radiation of electrons gyrating in a static magnetic field [1], [2]. Gyrotrons are capable of generating megawatt-level powers at high frequencies of the order of 10^2 GHz, and have wide applications [3], including radars, advanced telecommunication systems, technological processes, atmospheric sensing, extra-high resolution spectroscopy, etc. However, the main application motivating the research in gyrotrons is the electron cyclotron resonance heating of fusion plasmas in tokamaks and stellarators, as well as the noninductive current drive in tokamaks [4]–[6]. In order to design and implement efficient gyrotrons for fusion reactors, intensive theoretical, numerical, and experimental studies are taking place for the investigation of a variety of complex phenomena occurring in these devices. Among them, we can refer to mode competition [7, Ch. 5], hysteresis-like effects [8], and spatiotemporal chaos [9].

Most of the implemented numerical algorithms have heavy CPU-consuming parts spent in electron trajectory calculation via standard integration methods, such as the Runge–Kutta method. For these methods, small integration steps are required for an acceptable accuracy, leading to large computation times. Moreover, standard methods are not capable of taking into account several structural and physical properties of the motion equations. However, an efficient numerical model of electron motion has to preserve the properties of the system and take advantage of their existence in order to reduce the computation time.

In recent papers [10], [11], we have studied the complex electron dynamics in gyrotron resonators in the context of Hamiltonian formalism, and we have used the canonical perturbation method (CPM) in order to calculate approximate invariants of the system. The latter are used for the description of the electron phase space and the calculation of the electron distribution function. In this work, we show that the CPM can be used for the construction of a Hamiltonian map [12], [13], defined through the generating function of a canonical transformation, which describes the electron motion and can be used for efficient symplectic integration [14]–[16] of the electron equations of motion. The word "symplectic" comes from Greek meaning "twining or plaiting together," and is related to Hamiltonian systems, since the canonical coordinate and canonical momentum are intertwined by the symplectic two-dimensional form [12, p. 347]. In comparison with standard integration methods (such as Runge–Kutta), the symplectic integration [13, p.172] has several advantages: 1) it is a canonical map, preserving the Hamiltonian structure of the system, as well as the phase space volume and other integral invariants associated with Hamiltonian systems; 2) it takes into account the effective perturbation of electron motion due to the interaction with the radio-frequency (RF) field and its strong inhomogeneity in the phase space; 3) it can be iterated over larger intervals without significant deterioration of the accuracy; and 4) it can be extended to higher order via the Lie transforms method.

This paper consists of five sections. In Section II, the Hamiltonian formulation of the equations of electron motion is presented for the case of resonant electron interaction with a single RF mode at the first harmonic of the electron cyclotron frequency. Although the results that follow are directly applicable to the general case of interaction with multiple RF modes at any harmonic of the electron cyclotron frequency, the aforementioned case is used as an example for the presentation and the evaluation of our approach. The construction of the Hamiltonian map with utilization of the CPM is given in Section III for the general case of any RF field longitudinal profile. In Section IV, we focus on the case of the widely used Gaussian RF profile and present the results provided by iteration of the Hamiltonian map. The results are discussed and compared with the standard fourth-order Runge–Kutta method. Finally, the main conclusions are summarized in Section V.

Manuscript received September 20, 2005; revised March 7, 2006. This work was supported in part by the European Fusion Programme (EURATOM) and in part by the Greek General Secretariat of Research and Technology. The sponsors do not bear any responsibility for the contents in this work.

O. Dumbrajs is with the Department of Engineering Physics and Mathematics, Helsinki University of Technology, Association EURATOM-TEKES, FIN-02150 Espoo, Finland, and also with the Institute of Solid State Physics, University of Latvia, Kengaraga, LV-1063 Riga, Latvia.

Y. Kominis, K. A. Avramides, K. Hizanidis, and J. L. Vomvoridis are with the School of Electrical and Computer Engineering, National Technical University of Athens, Association EURATOM-Hellenic Republic, Zographou GR-15773, Greece (e-mail: gkomin@central.ntua.gr).

Digital Object Identifier 10.1109/TPS.2006.875763

II. Hamiltonian Formulation of the Model

As an example, let us consider the simple equation describing the electron motion in a gyrotron resonator, for the case of electron interaction with a single RF mode being in resonance at the first harmonic of the electron cyclotron frequency [7]

$$\frac{dp}{d\zeta} + i\left(\Delta + |p|^2 - 1\right)p = iFf(\zeta) \tag{1}$$

with the initial condition $p(\zeta_0) = \exp(i\theta_0), 0 \le \theta_0 \le 2\pi$. Here, p is the dimensionless transverse momentum of the electron, $\zeta = (\beta_{\perp 0}^2\omega/2\beta_{\|0}c)z$ is the dimensionless coordinate, $\beta_{\perp 0} = v_{\perp 0}/c$ and $\beta_{\|0} = v_{\|0}/c$ are the normalized transverse and parallel velocities of the electron at the entrance to the cavity, $\Delta = 2(\omega - \omega_c)/\beta_{\perp 0}^2\omega$ is the frequency mismatch, $\omega_c = (e/m)B/\gamma_{\rm rel}$ is the electron cyclotron frequency, B is the magnetic field in Tesla, $\gamma_{\rm rel} = 1 + (mc^2/e)^{-1}U$ is the relativistic factor, U is the accelerating voltage, F is the dimensionless beam to RF coupling factor. It should be noted that in the gyrotron literature one can find many alternatives to (1). However, only (1) represents the most compact form describing electron interaction with RF field in the cavity and is the most suitable for the Hamiltonian formulation. This equation was derived by Yulpatov as early as 1974 in the lectures [1], which are unavailable for Western readers. However this derivation has been reproduced in the recent book [7, Sec. 3.2, p. 51–57], where one can find all the details of derivation of the equation and its relation to explicit amplitudes of the electric and magnetic fields. The derivation method is based on the representation of the RF field acting upon a gyrating electron as a superposition of angular harmonics of waves rotating around the electron guiding center. This representation allows to distinguish the harmonic which is in resonance with the electron cyclotron motion, and average the equations of motion over fast gyrations.

Following [17], by representing p in Cartesian form $p = Q + iP$, the (1) is transformed to the following system of coupled differential equations:

$$\begin{aligned}\frac{dQ}{d\zeta} &= -\delta P + P(Q^2 + P^2) - Fg(\zeta)\\ \frac{dP}{d\zeta} &= +\delta Q - Q(Q^2 + P^2) + Fh(\zeta)\end{aligned} \tag{2}$$

where $\delta = 1 - \Delta$, $h(\zeta) = \mathrm{Re}[f(\zeta)]$, $g(\zeta) = \mathrm{Im}[f(\zeta)]$.

The set of (2) represents a one-degree of freedom, nonautonomous Hamiltonian system (the dimensionless position coordinate ζ can be regarded as time), with the Hamiltonian

$$\begin{aligned}H(Q,P,\zeta;F) = &-\frac{\delta}{2}(Q^2 + P^2)\\ &+\frac{1}{4}(Q^2 + P^2)^2 - F\left(Qh(\zeta) + Pg(\zeta)\right).\end{aligned} \tag{3}$$

The system (2) can be considered as a autonomous system in the extended phase space $(P, -H, Q, \zeta)$, where $-H$ and ζ are treated as momentum and coordinate in a four-dimensional phase space (two-degrees of freedom system). The flow is parameterized by new "time" t and the new Hamiltonian has the form [12], [13]

$$\hat{H}(P, -H, Q, \zeta) = H(P, Q, \zeta) - H. \tag{4}$$

The new Hamiltonian $\hat{H}$ does not depend explicitly on the new "time" t and thus, it is a constant of the motion. However, the existence of a second constant of the motion is required so that the system is integrable, but this is not expected in the general case. Only a few special RF field profiles $f(\zeta)$ result in the existence of a second constant of the motion, such as $f(z) = \exp(ik\zeta)$ [17], so that in general the system is considered as nonintegrable.

In order to apply the CPM and construct the Hamiltonian map, of the nonintegrable system we can start from an integrable system which differs from the actual one in terms of a small parameter and consider the actual system as a perturbation of the integrable one (near-integrable). In our case, the unperturbed (integrable) system can be defined as the one which describes the electron motion in the absence of the RF field, with Hamiltonian

$$H_0(P,Q) = H(P,Q,\zeta;F=0) = -\frac{\delta}{2}(Q^2+P^2) + \frac{1}{4}(Q^2+P^2)^2. \tag{5}$$

For this system, the Hamiltonian H_0 does not depend explicitly on time, and represents the conserved energy of the electrons under no interaction with an RF field. The Hamiltonian of the perturbed system can be written in the following form:

$$H(P,Q,\zeta;F) = H_0(P,Q) + H_1(P,Q,\zeta;F) \tag{6}$$

where $H_1(P,Q,\zeta;F) = -F(Qh(\zeta) + Pg(\zeta))$ is the perturbative term representing the presence of the RF field. The coupling factor F can be considered as the small parameter in the perturbation approach which follows. From a physical point of view, a small F is required in order to preserve the gyrating character of the electron motion.

Starting from the unperturbed system, we transform the original variables (P, Q) to action-angle variables (J, θ) [12]

$$\begin{aligned}J &= \frac{P^2 + Q^2}{2}\\ \theta &= \arcsin\left(\frac{Q}{\sqrt{P^2 + Q^2}}\right).\end{aligned} \tag{7}$$

The transformed Hamiltonian has the form

$$H_0(J) = J^2 - \delta J \tag{8}$$

and the electron gyration frequency is given by

$$\omega_\theta = \frac{\partial H_0(J)}{\partial J} = 2J - \delta. \tag{9}$$

The Hamiltonian of the perturbed (near-integrable) system can be written in terms of the action-angle variables of the unperturbed system as follows:

$$H(J,\theta,\zeta;F) = H_0(J) + H_1(J,\theta,\zeta;F) \tag{10}$$

where $H_0(J)$ is given in (8) and

$$H_1(J,\theta,\zeta;F) = F\sqrt{2J}\mathrm{Im}\left\{\exp(i\theta)f(\zeta)\right\}. \tag{11}$$

The aperiodic dependence of the perturbation term on the time ζ differentiates the topology of the flow in the extended phase space, with respect to other cases [10]: instead of the usual tori ($(J,\theta,\zeta) \in \mathbb{R}\times\mathbb{T}^2$) resulting from time-periodic perturbations, we deal with infinite cylinders ($(J,\theta,\zeta) \in \mathbb{R}\times\mathbb{T}\times\mathbb{R}$).

III. Construction of the Hamiltonian Map

According to the Hamilton–Jacobi theory [12], the solution of a Hamiltonian system can be given in terms of a canonical transformation from a set of a canonical variables (J,θ) to a new set of constant quantities $(\bar{J},\bar{\theta})$, for which the new Hamiltonian $\bar{H}(\bar{J})$ is a function of the new action only. In this set, the equations of motion have the simple solution

$$\begin{aligned}\frac{d\bar{J}}{d\zeta} &= -\frac{\partial\bar{H}}{\partial\bar{\theta}} = 0, \quad \bar{J} = \text{const.}\\ \frac{d\bar{\theta}}{d\zeta} &= \frac{\partial\bar{H}}{\partial\bar{J}} = \bar{\omega}(\bar{J}), \quad \bar{\theta} = \bar{\omega}(\bar{J})\zeta + \bar{\theta}_0.\end{aligned} \tag{12}$$

With such a transformation, the equations of the transformation relating the old and the new canonical variables, along with the solution (12) give explicitly the solution of the system. The generating function $S(\bar{J},\theta)$ of the transformation, is given by the solution of the Hamilton–Jacobi equation

$$H\left(\theta,\frac{\partial S}{\partial\theta},\zeta\right) + \frac{\partial S}{\partial\zeta} = \bar{H}(\bar{J}). \tag{13}$$

For the case of integrable systems, this partial differential equation is completely separable, with each independent invariant of the motion corresponding to a separation constant for each one of the degrees of freedom. For nonintegrable systems, such as the system describing electron motion, the Hamilton–Jacobi equation can be solved approximately via the CPM [12]. In order to obtain an approximate solution of (13), we expand both the generating function $S(\bar{J},\theta)$ and the new Hamiltonian $\bar{H}(\bar{J},\bar{\theta})$ in power series of a small parameter ϵ (ϵ is the ordering parameter of the perturbation method, which can be set equal to 1 at the end of the calculations)

$$S = \bar{J}\theta + \epsilon S_1 + \ldots \tag{14}$$

$$\bar{H} = \bar{H}_0 + \epsilon\bar{H}_1 + \ldots \tag{15}$$

where the lowest-order term has been chosen to generate the identity transformation $J = \bar{J}$ and $\bar{\theta} = \theta$. Using the canonical transformation equations, the old action and angle can be also expressed as power series in ϵ

$$J = \bar{J} + \epsilon\frac{\partial S_1(\bar{J},\theta,\zeta)}{\partial\theta} + \cdots \tag{16}$$

$$\bar{\theta} = \theta + \epsilon\frac{\partial S_1(\bar{J},\theta,\zeta)}{\partial\bar{J}} + \cdots \tag{17}$$

and the new Hamiltonian is

$$\bar{H}(\bar{J},\bar{\theta},\zeta) = H(J,\theta,\zeta) + \frac{\partial S(\bar{J},\theta,\zeta)}{\partial\zeta}. \tag{18}$$

Inserting these equations into (18) and equating like powers of ϵ, we have to zero order

$$\bar{H}_0 = H_0(\bar{J}) \tag{19}$$

and to first order

$$\bar{H}_1 = \frac{\partial S_1}{\partial\zeta} + \omega_\theta\frac{\partial S_1}{\partial\bar{\theta}} + H_1 \tag{20}$$

where $\omega_\theta = \partial H_0/\partial J$.

The appropriate choice of $\bar{H}_1$ incorporates all the essential terms coming from H_1, which yield nonphysical expressions for the generating function (and the corresponding near-identity transformation), when integrated along unperturbed orbits. Such expressions may not respect the periodicity of the original system or may not remain bounded (for example, a constant term in H_1 would result in an S_1 which increases infinitely with ζ), so that the ordering of the perturbation method is destroyed. However, the specific form of H_1, in our case, does not result in such expressions, as will be shown, so that $\bar{H}_1$ can be set equal to zero. Thus, the first order equation, is written in the following form:

$$\frac{\partial S_1}{\partial\zeta} + \omega_\theta\frac{\partial S_1}{\partial\bar{\theta}} = -H_1. \tag{21}$$

The solution of (21) in the interval (ζ_k,ζ_{k+1}) is given by

$$S_1(\bar{J},\theta,\zeta_{k+1},\zeta_k) = S_1(\bar{J},\theta,\zeta_{k+1},-\infty) - S_1(\bar{J},\theta,\zeta_k,-\infty) \tag{22}$$

where

$$S_1(\bar{J},\theta,\zeta,-\infty) = F\sqrt{2\bar{J}}\mathrm{Im}\left\{e^{i\theta}\int_{-\infty}^{\zeta} f(t)e^{i\omega_\theta(t-\zeta)}dt\right\}. \tag{23}$$

This generating function can be used in (16) and (17) (with $\epsilon \equiv 1$), in order to define the Hamiltonian map $(J_k, \theta_k) \rightarrow (J_{k+1}, \theta_{k+1})$

$$J_{k+1} = J_k - \frac{\partial S_1(J_{k+1}, \theta_k, \zeta_{k+1}, \zeta_k)}{\partial \theta_k}$$
$$\theta_{k+1} = \theta_k + \frac{\partial S_1(J_{k+1}, \theta_k, \zeta_{k+1}, \zeta_k)}{\partial J_{k+1}} \tag{24}$$

which governs the evolution of the system from ζ_k to ζ_{k+1}. The map equation providing the action at each step is a nonlinear implicit equation with respect to the action. According to the fixed point theorem, this equation has a unique solution provided that

$$\left| \frac{\partial^2 S_1}{\partial J_{k+1} \partial \theta_k} \right| < 1. \tag{25}$$

This condition relates the maximum iteration step $\Delta z = z_{k+1} - z_k$ allowable for unique solution, to the perturbation and its parameters. The solution can be obtained by utilizing a standard Newton–Raphson method.

This map is quite general since it holds for any RF field profile $f(\zeta)$. The latter can be either a fixed profile in the context of the cold-cavity approximation or a self-consistent profile, obtained at some iteration step of a self-consisted algorithm which contains both electron motion equation and wave equation for the RF field. In all cases, the Hamiltonian map can be used for efficient calculation of electron trajectories. Moreover, the application of Hamiltonian map (24) can be directly extended to the general case of electron interaction with multiple RF modes at any harmonic of the electron cyclotron frequency. By utilizing the first order generating function obtained in [11], the definition of the corresponding Hamiltonian map is straightforward. Also, higher accuracy of the map can be achieved by calculation of higher order generating functions through the CPM. The Lie transforms method can be utilized for simplifying the procedure of higher order CPM.

IV. Results and Discussion

Before applying the Hamiltonian map, let us discuss the efficiency of standard methods. It is well known that the Runge–Kutta method ignores the structural and physical properties of the system, and it fails in conserving several invariant quantities and properties, related to symmetries of the system. In a Hamiltonian system, the method fails to conserve the phase space volume of an ensemble of initial conditions, since the numerical integration process introduces a non-Hamiltonian perturbation, resulting in an effective dissipation. In contrast, the Hamiltonian map, by arranging each integration step to be a canonical transformation, it preserves not only the phase space volume, but all the Poincare invariants [12], [14] related to the Hamiltonian structure of the system. These integral invariants comprise integrals over subspaces of the phase space of different dimensions, and form a sequence with the phase space volume integral being its final member. This property of the Hamiltonian map is quite important for electron trajectory calculations involved in gyrotrons, since the collective dynamical behavior of an ensemble of initial conditions, related to electrons of a beam, is of interest.

In the following, we apply the Hamiltonian map (24) for the calculation of electron trajectories in the case of a Gaussian RF field longitudinal profile:

$$f(\zeta) = \exp\left[-\left(\frac{2\zeta}{\mu} - \sqrt{3} \right)^2 \right] \tag{26}$$

where $\mu = \pi(\beta_{\perp 0}^2/\beta_{\|0})L/\lambda$ is the dimensionless length of the resonator with length L. For the specific form (26) of the RF field profile, the first order generating function, as obtained from (23) is the following:

$$S_1(\bar{J}, \theta, \zeta, -\infty) = \mathrm{Im}\left\{ \frac{\sqrt{\pi}}{4} F\mu\sqrt{2\bar{J}} e^{i\theta} e^{-i\omega_\theta(\bar{J})(\zeta - \sqrt{3}\mu/2)} \right.$$
$$\left. \times e^{-\left(\frac{\omega_\theta(\bar{J})\mu}{4}\right)^2} \left[1 + \mathrm{erf}\left(\frac{8(\zeta - \sqrt{3}\mu/2) - i\omega_\theta(\bar{J})\mu^2}{4\mu} \right) \right] \right\}. \tag{27}$$

The perturbation strength is shown to be proportional to the product of the coupling factor with the cavity length ($\sim F\mu$), while cavity length (μ) determines the width of the localized resonant action area where strong interactions occur, as shown in the exponential term. Shorter resonator lengths (μ) result in wider resonant areas in the phase space. The frequency mismatch Δ determines the center of the resonant area through the relation $J_c = (1 - \Delta)/2$. Also, the last term represents the transient evolution of electron dynamics, and becomes constant for large ζ.

The Hamiltonian map is obtained by substituting (27) in (22) and (24). The map is applied for a variety of perturbation strengths ($\sim F\mu$) and initial conditions, and the results are compared to those obtained by numerical integration of motion equations (2) utilizing a standard fourth-order Runge–Kutta method. The values $\Delta = 0.5$, $\mu = 15$ are considered in the following examples. In Figs. 1(a) and (b), Fig. 2(a) and (b), and Fig. 3(a) and (b), the Poincare surface of section (J, θ) at $\zeta_o = 30$, is shown for $F = 0.01, 0.05, 0.1$, respectively. The initial conditions consist of $N = 500$ angle values θ uniformly distributed in the interval $[0, 2\pi]$, for each initial action value $J = 0.1, 0.2, \ldots, 0.8$. For the results obtained through the Runge–Kutta method $n_1 = 1000$ integration steps were used, while only $n_2 = 50$ steps were used for the Hamiltonian map iteration. In all cases, the results are in excellent agreement. The significantly smaller number of steps (20 times!) of the Hamiltonian map iteration, as well as its volume preservation property, are the main advantages of this method. In all cases the Poincare surface of section consists of resonant areas where the initial action value results in strong interaction, while outside these areas the electron motion is practically unperturbed by the presence of the RF field. The width of the resonant areas, increases with F for a given value of μ. Note that for $F = 0.05$ (Fig. 2), there is no significant action variation for electrons having an initial action of $J = 0.5$, while for higher perturbation $F = 0.1$ (Fig. 3), these electrons undergo large action

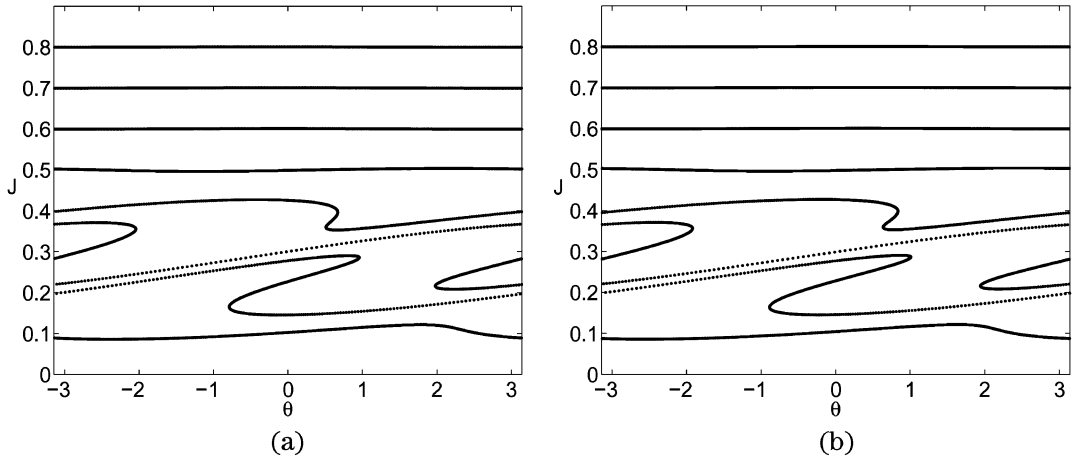

Fig. 1. Poincare surfaces of section at $\zeta_o = 30$, for $F = 0.01, \mu = 15, \Delta = 0.5$. Initial conditions consist of $N = 500$ angle values θ uniformly distributed in the interval $[0, 2\pi]$, for each initial action value $J = 0.1, 0.2, \ldots, 0.8$. (a) Fourth-order Runge–Kutta method, $n_1 = 1000$ steps. (b) Hamiltonian map, $n_2 = 50$ steps.

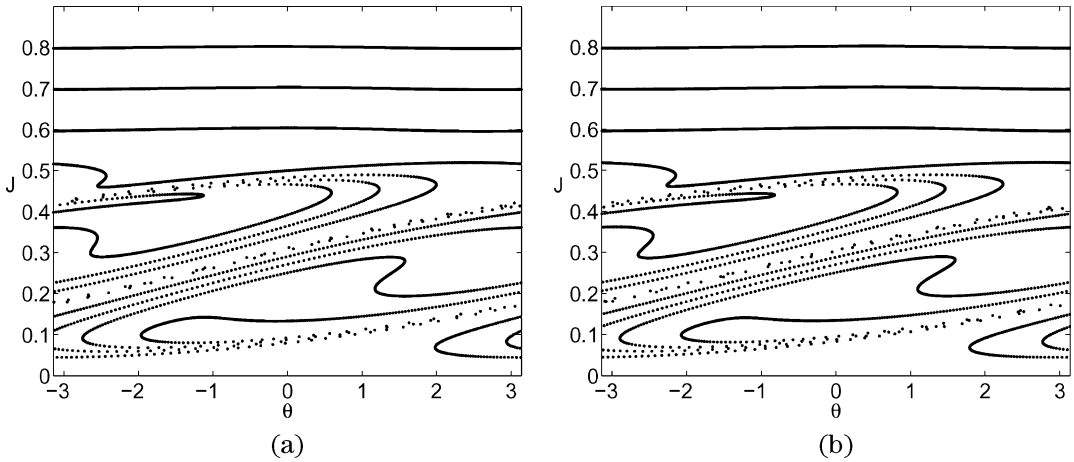

Fig. 2. Poincare surfaces of section at $\zeta_o = 30$, for $F = 0.05, \mu = 15, \Delta = 0.5$. Initial conditions consist of $N = 500$ angle values θ uniformly distributed in the interval $[0, 2\pi]$, for each initial action value $J = 0.1, 0.2, \ldots, 0.8$. (a) Fourth-order Runge–Kutta method, $n_1 = 1000$ steps. (b) Hamiltonian map, $n_2 = 50$ steps.

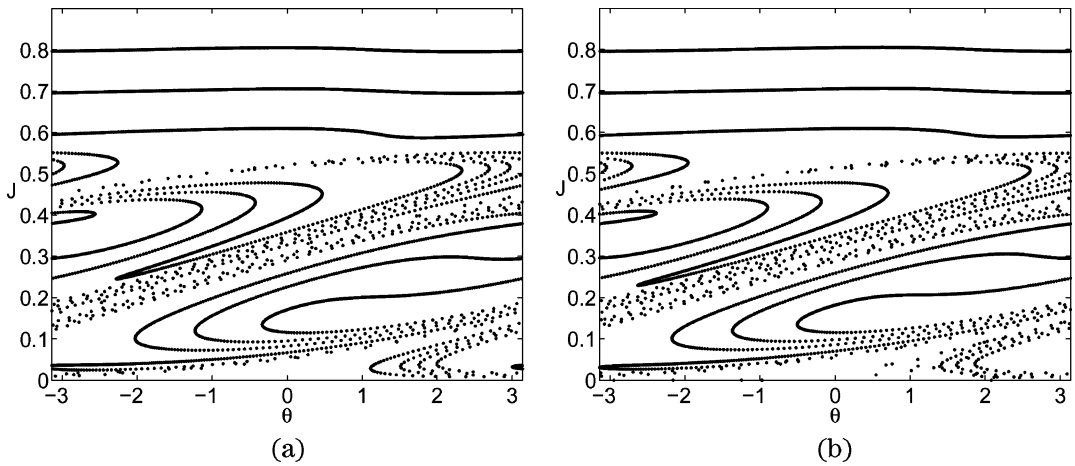

Fig. 3. Poincare surfaces of section at $\zeta_o = 30$, for $F = 0.10, \mu = 15, \Delta = 0.5$. Initial conditions consist of $N = 500$ angle values θ uniformly distributed in the interval $[0, 2\pi]$, for each initial action value $J = 0.1, 0.2, \ldots, 0.8$. (a) Fourth-order Runge–Kutta method, $n_1 = 1000$ steps. (b) Hamiltonian map, $n_2 = 50$ steps.

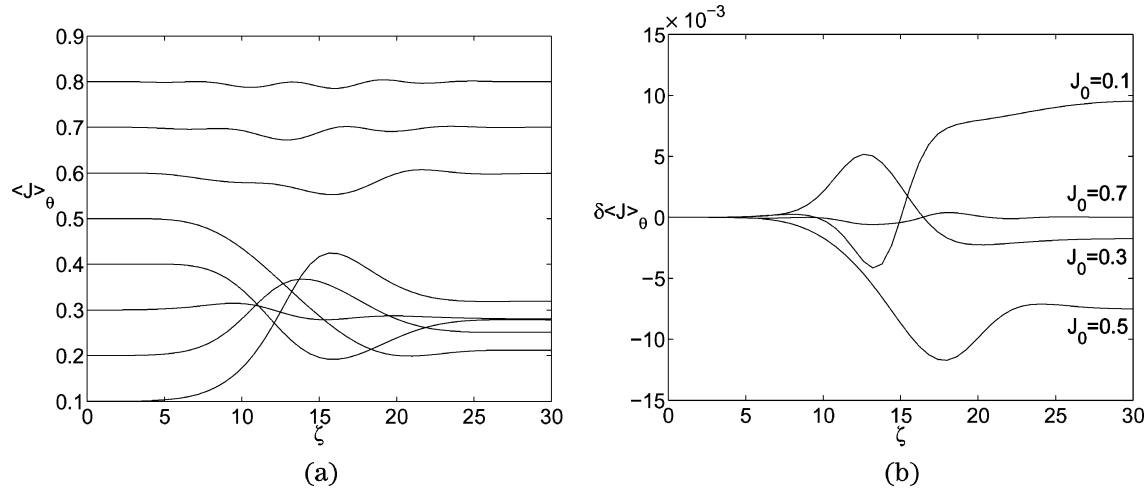

Fig. 4. (a) Angle-averaged action variation $\langle J\rangle_\theta$ (Hamiltonian map, $n_2 = 50$ steps). (b) Difference between $\langle J\rangle_\theta$, as calculated through Runge–Kutta method ($n_1 = 1000$ steps) and Hamiltonian map ($n_2 = 50$ steps).

variations. However, in contrast to the action variation which is bounded in the resonant area, the angle undergoes unbounded variations resulting in the complex folding of the lines shown in the Poincare surfaces of section, for strong perturbation: two electrons, corresponding to the same initial action and different neighboring initial angles, end up with different actions after exiting the RF field; since the frequency ω_θ is action dependent (9), these electrons rotate with different frequencies and their angles continuously diverge as ζ increases. However, in all calculations involved in gyrotron simulation numerical algorithms, the exact angle of the electrons is not of interest and averaging of action variation with respect to the angle is involved. The latter is related to the energy transfer from the electron beam to the RF field and it determines the gyrotron efficiency.

The averaged action variation with respect to the angle $\langle J\rangle_\theta = (1/N)\sum_{k=1}^{N} J_k$ is shown in Fig. 4(a), for the case corresponding to Fig. 3, as obtained from iteration of the Hamiltonian map (24). For all initial action values, $\langle J\rangle_\theta$ becomes constant for large ζ, since the action variation is localized within the characteristic width of the Gaussian profile (related to cavity length). Initial actions located in the lower half of the resonant area ($J = 0.1, 0.2$) result in averaged action increasing, while decreasing of $\langle J\rangle_\theta$ occurs for initial actions located in the upper half ($J = 0.4, 0.5$). Close to the center ($J = 0.3$) and outside ($J = 0.6, 0.7, 0.8$) the resonant area, electron interaction with the RF field results in practically zero averaged action variation. The difference $\delta\langle J\rangle_\theta$ between calculating $\langle J\rangle_\theta$, by utilization of the Hamiltonian map ($n_2 = 50$ steps) and the Runge–Kutta method ($n_1 = 1000$ steps), is shown in Fig. 4(b). The maximum differences at $\zeta = 30$ are less than 10^{-2} and correspond to initial action values located inside the resonant area and close to the boundaries. For initial action values close to the center of the resonant area or outside of it, the difference is less than 10^{-3}.

It is worth mentioning that for nonresonant initial action values as well as for the case of small perturbation strengths even less iteration steps of the Hamiltonian map ($n_2 < 20$) can provide accurate calculation of the trajectories as well as the averaged action variation. Since the locations and widths of the resonant areas are predicted by the generating function in terms of parameters (F, μ, Δ) of the perturbation, an efficient algorithm can use this information in order to adjust the size of iteration steps according to the effective perturbation strength for each case of initial conditions and parameters. The effective perturbation strength depends on both the parameter set and the relative position of the initial conditions with respect to the resonant phase space areas. Thus, the minimum number of steps can be used for each set of initial conditions corresponding to an electron beam (electrons with the same action and different angles), resulting in a significant performance increase of the algorithm calculating the electron trajectories.

Finally, let us illustrate the advantages of the Hamiltonian mapping approach for the operating parameter set $\mu = 17$, $F = 0.12$, $\Delta = 0.50$ corresponding to maximum perpendicular efficiency $\eta_\perp$ [7]

$$\eta_\perp = 2\,\langle 0.5 - J(\zeta_o)\rangle_\theta\,. \tag{28}$$

The Poincare surfaces of section for the initial action value $J = 0.5$ are shown in Fig. 5(a) and (b), as obtained with utilization of the fourth-order Runge–Kutta method with $n_1 = 1000$ steps and the Hamiltonian map with $n_2 = 150$ steps, respectively. The two figures are quite similar. However, the advantage of the Hamiltonian mapping method is shown in Fig. 6 where the calculated efficiency (28) as a function of the number of iterations is depicted, for the two methods. We find that for the Hamiltonian mapping method the calculated value becomes almost constant with respect to the number of iterations (i) for $i > 100$, while for the Runge–Kutta method, the calculated value converges very slowly to the value of the first method, for large number of iterations.

V. Conclusion

Electron dynamics in gyrotron resonators can be described in terms of a Hamiltonian mapping constructed via the CPM. This map incorporates the dependency of electron dynamics on the parameters of the interacting RF field and it can be used for

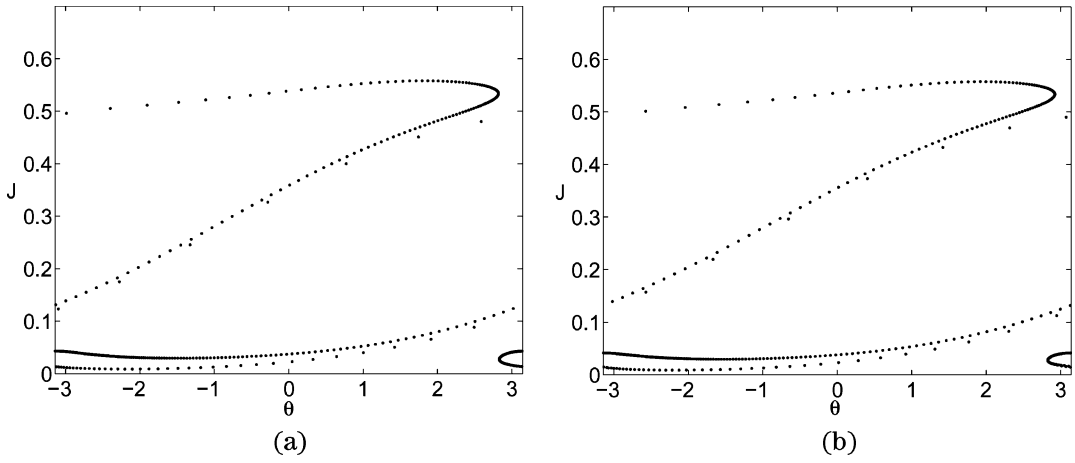

Fig. 5. Poincare surfaces of section at $\zeta_o = 30$, for an initial action value $J = 0.5$ and a parameter set corresponding to maximum efficiency $F = 0.12$, $\mu = 17$, $\Delta = 0.5$. Initial conditions consist of $N = 500$ angle values θ uniformly distributed in the interval $[0, 2\pi]$. (a) Fourth-order Runge–Kutta method. $n_1 = 1000$ steps. (b) Hamiltonian map, $n_2 = 150$ steps.

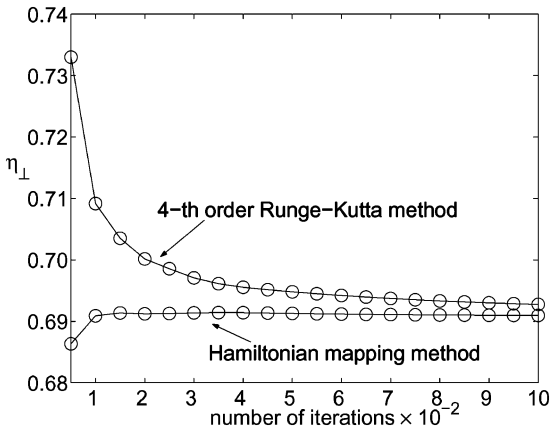

Fig. 6. Efficiency calculation (28) versus number of iterations for a parameter set corresponding to maximum efficiency $F = 0.12$, $\mu = 17$, $\Delta = 0.5$, as obtained with utilization of the fourth-order Runge–Kutta and the Hamiltonian mapping method.

trajectory calculations, through successive iteration, resulting in a symplectic integration scheme. The direct relation of the map to the physics of the model, along with its canonical form (phase space volume preserving) and the significant reduction of the number of iteration steps required for acceptable accuracy, are the main advantages of this method in comparison with standard methods such as Runge–Kutta.

The general form of the Hamiltonian map allows for wide applications as a part of several numerical algorithms which incorporate CPU-consuming electron trajectories calculations. In a self-consistent approach, the Hamiltonian map technique can still be used for the calculation of electron trajectories, while in this case, the number of required iterations would depend, not only on the desired accuracy of the electron output momenta, but also on the required accuracy of the RF field profile, as derived from the corresponding equations. Finally, the method can also be applied to other microwave sources and devices, where wave–particle interactions occur.

REFERENCES

[1] V. A. Flyagin, A. V. Gaponov, M. I. Petelin, and V. K. Yulpatov, "The gyrotron," *IEEE Trans. Microwave Theory Tech.*, vol. MTT-25, no. 6, p. 514, Jun. 1977.

[2] B. G. Danly and R. J. Temkin, "Generalized nonlinear harmonic gyrotron theory," *Phys. Fluids*, vol. 29, p. 561, 1986.

[3] T. Idehara, S. Mitsudo, R. Pavlichenko, I. Ogawa, D. Wagner, and M. Thumm, "Development of submillimeter wave gyrotron FU series," in *Proc. Int. Workshop*, Nizhny Novgorod, Russia, Aug. 1–9, 2002, p. 116.

[4] G. G. Denisov, "Megawatt gyrotrons for fusion research. The state of the art and trends of development, strong microwaves in plasmas," in *Proc. Int. Workshop*, Nizhny Novgorod, Russia, Aug. 1–9, 2002, p. 29.

[5] G. Dammertz, S. Alberti, A. Arnold, E. Borie, V. Erckmann, G. Gantenbein, E. Giguet, R. Heidinger, J. P. Hogge, S. Illy, W. Kasparek, K. Koppenburg, M. Kuntze, H. P. Laqua, G. LeCloarec, Y. LeGoff, W. Leonhardt, C. Lievin, R. Magne, G. Michel, G. Mueller, G. Neffe, B. Piosczyk, M. Schmid, K. Schwoerer, M. K. Thumm, and M. Q. Tran, "Development of a 140-GHz 1-MW continuous wave gyrotron for the W7-X stellarator," *IEEE Trans. Plasma Sci.*, vol. 30, no. 3, pp. 808–818, Jun. 2002.

[6] B. Piosczyk, G. Dammertz, O. Dumbrajs, O. Drumm, S. Illy, J. Jin, and M. Thumm, "A 2-MW, 170-GHz coaxial cavity gyrotron," *IEEE Trans. Plasma Sci.*, vol. 32, no. 2, pp. 413–417, Apr. 2004.

[7] G. S. Nusinovich, *Introduction to the Physics of Gyrotrons*. Baltimore, MD: Johns Hopkins Univ. Press, 2004.

[8] O. Dumbrajs, T. Idehara, Y. Iwata, S. Mitsudo, I. Ogawa, and B. Piosczyk, "Hysteresis-like effects in gyrotron resonators," *Phys. Plasmas*, vol. 10, p. 1183, 2003.

[9] M. I. Airila and O. Dumbrajs, "Spatio-temporal chaos in the transverse section of gyrotron resonators," *IEEE Trans. Plasma Sci.*, vol. 30, no. 3, pp. 846–850, Jun. 2002.

[10] Y. Kominis, O. Dumbrajs, K. A. Avramides, K. Hizanidis, and J. L. Vomvoridis, "Chaotic electron dynamics in gyrotron resonators," *Phys. Plasmas*, vol. 12, p. 043104, 2005.

[11] ——, "Canonical perturbation theory for complex electron dynamics in Gyrotron resonators," *Phys. Plasmas*, vol. 12, 2005, 113102.

[12] H. Goldstein, *Classical Mechanics*, 2nd ed. Reading, MA: Addison Wesley, 1980.

[13] A. J. Lichtenberg and M. A. Lieberman, *Regular and Chaotic Dynamics*. New York: Springer-Verlag, 1992.

[14] P. J. Channel and S. Scovel, "Symplectic integration of Hamiltonian systems," *Nonlinearity*, vol. 3, p. 231, 1990.

[15] S. S. Abdullaev, "A new integration method of Hamiltonian systems by symplectic mappings," *J. Phys. A, Math. Gen.*, vol. 32, p. 2745, 1999.

[16] ——, "The Hamilton-Jacobi method and Hamiltonian maps," *J. Phys. A, Math. Gen.*, vol. 35, p. 2811, 2002.

[17] M. I. Airila, O. Dumbrajs, A. Reinfelds, and D. Teychenne, "Traces of stochasticity in electron trajectories in gyrotron resonators," *Int. J. Infrared Millim. Waves*, vol. 21, p. 1759, 2000.

Olgierd Dumbrajs (SM'99) was born in Riga, Latvia. He received the B.S. degree in theoretical physics from Latvian State University, Riga, Latvia, in 1965, and the Ph.D. degree in theoretical particle physics from Moscow State University, Moscow, U.S.S.R. (now Russia), in 1971.

From 1971 to 1985, he was with the Joint Institute for Nuclear Research, Dubna, U.S.S.R., and at several European Nuclear Research Centers. At that time, he published many papers on nuclear and particle physics. In 1985, he joined the Gyrotron Project at the Forschungszentrum Karlsruhe, Karlsruhe, Germany. Since 1993, he has been a special research worker with the Academy of Finland and with the Helsinki University of Technology. He is a Professor at the Transport and Telecommunication Institute of Latvia, Riga. His current research interests are in the field of gyrotron theory, nonlinear dynamics, and plasma physics. In 2005, he received a special EURATOM grant to carry out research on the topic "stochastization of magnetic fields and magnetic reconnection."

Dr. Dumbrajs is a life member of the American Physical Society. In 2001, he was elected a foreign member of the Latvian Academy of Sciences.

Yannis Kominis was born in Athens, Greece, on December 28, 1973. He received the Dipl.Eng. degree and the Ph.D. degree from the School of Electrical and Computer Engineering, National Technical University of Athens (NTUA), Athens, Greece, in 1997 and 2004, respectively.

Since 2004, he has been a Postdoctoral Researcher in the Plasmas, Electron Beam and Non-Linear Optics Laboratory, NTUA. His basic research interests are in complex dynamics of nonlinear wave-particle interactions, with applications to plasma physics and generation of high-power microwaves, solitons and nonlinear wave propagation in plasma and optical systems.

Dr. Kominis is a member of the Technical Chamber of Greece.

Konstantinos A. Avramides was born in Athens, Greece, on April 29, 1971. He received the Dipl. Piano Soloist degree from the National Conservatory, Athens, Greece, in 1995, and the Dipl.Eng. degree, in 1998, from the School of Electrical and Computer Engineering, National Technical University of Athens, Athens, Greece, where he is currently working toward the Ph.D. degree in the Plasmas, Electron Beam and Non-Linear Optics Laboratory.

He has been a Research Assistant in the Plasmas, Electron Beam and Non-Linear Optics Laboratory, National Technical University of Athens, since 1999. From 1997 to 1998, he was with the National Service. His research interests concentrate in the design and numerical simulation of coaxial and harmonic gyrotrons.

Mr. Avramides is a member of the Technical Chamber of Greece.

Kyriakos Hizanidis received the M.Eng. degree in mechanical and electrical engineering from the School of Electrical and Computer Engineering, the National Technical University of Athens, Athens, Greece, in 1975 and the Ph.D. degree in fusion plasma physics from the Massachusetts Institute of Technology, Cambridge, in 1982.

He is currently a Professor at the School of Electrical and Computer Engineering, the National Technical University of Athens. His research interests include plasma kinetic theory, transport, instabilities, heating and current drive as well as nonlinear optics, solitons, and dynamical systems.

John L. Vomvoridis was born in Thessaloniki, Greece, on March 12, 1947. He received the Diploma in mechanical and electrical engineering from the National Technical University of Athens, Athens, Greece, in 1970, and the Ph.D. degree in plasma physics from Northwestern University, Evanston, IL, in 1977

He has worked at Northwestern University, the Naval Research Laboratory, Mission Research Corporation, and the Ministry of Research and Technology of Greece, and in 1984, he joined the faculty of the Department of Electrical and Computer Engineering, National Technical University of Athens, Greece, where he has served as a Professor in electromagnetic fields since 1991. His primary research interests are in interactions of electromagnetic fields with plasmas and electron beams, in particular in relation to the generation of high-power microwaves, including pioneering work on the quasi-optical gyrotron, the cyclotron auto-resonant maser, and the cyclotron resonance maser with anomalous Doppler shift.